Drop impact onto suspended and surface-attached metallic meshes: liquid penetration and spreading

C. Boscariol[1,2*], D. Sarker[3], S. Chandra[4], C. Crua[1,2], M. Marengo[1,2]

[1]Advanced Engineering Centre, University of Brighton, United Kingdom
[2]*School of Computing, Engineering and Mathematics, University of Brighton, BN2 4GJ Brighton, UK*
[3]School of Pharmacy and Biomolecular Science, University of Brighton, *BN2 4GJ Brighton*, UK
[4] Faculty of Applied Science & Engineering, University of Toronto, Canada
*Corresponding author: c.boscariol@brighton.ac.uk

Abstract

The interaction between drops and porous matter has important applications in many fields such as painting, paper coating, filtration and drug delivery, the latter considering for example reconstructive surgery processes. Since the phenomenon of drop impact onto a porous surface is particularly complex, a first step consists in analysing impacts on 2D deterministic structures, such as metallic meshes. The present paper shows the cases of (i) drop impacts onto meshes attached to a solid substrate and (ii) drop impacts onto the same meshes but suspended without substrate. By analysing the impact of droplets of water, acetone and a mixture of glycerol and water on meshes with different pore sizes, three main outcomes were observed for both test cases: deposition, partial imbibition and penetration. A higher amount of liquid penetration is linked to a higher velocity impact, lower viscosity and a larger dimension of the pore size. An estimation of the liquid penetration is given in order to evaluate the impregnation properties of the meshes. For the case of attached meshes, a map of the regimes is proposed.

Keywords: Drop impact, porous surface, metallic mesh, impact regimes, imbibition

Introduction

The phenomenon linked to droplet impact on porous surfaces has important applications in many fields. Some of the principal applications are given for example by the infiltration of rain drops and surface water into soil or the migration of oil in permeable porous media, which are both important subjects in environmental science [1]. Agrochemicals are typically distributed on plants by spraying them onto leaf surfaces into which they penetrate [2]. Furthermore, porous surfaces find application in internal combustion engines as it is possible to enhance fuel vaporization by spraying fuel droplets on a porous coating on the piston wall [3]. Droplet impact dynamics can affect the outcome in cell printing [4]. Moreover, the quality of images produced by ink-jet printing depends on the penetration and spreading of ink droplets landing on paper [5]. Suppression of fires by sprinkler systems involves droplets impinging on burning porous materials, such as wood [6]. The understanding of the most important parameters which play a major role in the evolution of the droplet inside the pore is still an open question. Roisman et al. [7] developed a model describing the different regimes of splashing thresholds, comparing the impact of droplet on porous and rough surface. The model they presented shows that in the case of porous surfaces a deposition outcome, without splash, will be enhanced by the partial penetration of the liquid in the pore. They proposed an experimental map showing that the two most significant parameters influencing the prompt splash-deposition are the Weber number and the ratio given by two geometrical characteristics linked to roughness. Yamamoto et al. [8] investigated droplet impact on textured surface fabricated by aligning stainless-steel razor blades in parallel. Focusing on a range of We number between 5 and 10, they observed partial penetration of liquid into the gaps between the blades, due to the collapse of the air cavity at the centre of the recoiling droplet. Neyval et al. [9] presented a numerical model, based on the finite volume method, to analyse the dynamics of the impact absorption of a liquid droplet impinging on a porous medium. By enhancing the effects of surface tension and capillary forces, they found a good agreement with experimental data. Sahu et al. [10] analysed the impact of nanoparticle suspension into porous filter membranes. They focused on penetration given by the hydrodynamic effect, which is due to the kinetic energy brought by a drop impacting on the porous media having a very small pore size with respect to drop size. By comparing this aspect with the effects given by dynamic and capillary pressures, they concluded that penetration into porous medium is possible not only when the dynamic pressure is higher than the capillary pressure, but also when hydrodynamic focusing, occurring when the drop diameter is much larger than pore diameter, is observed. Lorenceau et al. [11] analysed the impact of droplet on thin perforated plates. They pointed out at a critical speed above which the droplet is not entirely captured by the plate, but passes through it. Delbos et al. [12] investigated how an impacting drop can be forced into a capillary tube and observed a variety of regimes of droplet rebound or penetration for different combinations of impact velocity, tube radius and wetting condition.

The objective of this study was to develop our fundamental understanding of the interaction between droplets and complex porous surfaces, with and without attachment onto a rigid substrate. To achieve this we observed the

impact of liquid droplets on metal meshes in two different configurations in order to obtain a map to separate the different regimes in the first case, and estimate the impregnation properties of the mesh in the second case. In the first configuration, the square meshes were bonded to a flat, solid plate made of stainless steel, in the second configuration they were suspended using a purpose-built ring. This represents a structured porous surface that can be characterised by two parameters, mesh wire diameter and pore width, both of which were varied. In both configurations, experiments were done for different combinations of impinging drop radius, impact velocity, liquid surface tension and viscosity. Droplet impacts were recorded using a high-speed video camera and the final state of the droplet observed. Several different outcomes were seen, including: a portion of the liquid penetrating into the pores; all of the liquid penetrating; and deposition of the droplet onto the mesh. For the case of the attached meshes, dimensionless maps were developed to predict conditions under which each outcome occurred.

Experimental Methods

The experimental analysis was conducted using target surfaces selected from a set of stainless steel metal meshes used for filtration applications, with pore sizes varying from 25 and 400 µm (Plastok® Meshes and Filtration Ltd., Birkenhead, Merseyside, UK). Fig. 1 shows a sample of a scanning electron microscope (SEM) image of a mesh with 25 µm wire diameter and 25 µm pores, and 220 µm wire diameter and 400 µm pores (samples 1 and 8, respectively). Three liquids were used: water, acetone and a glycerol-in-water solution composed of 20% of water and 80% of glycerol (by volume), to analyse the effect of liquid viscosity and surface tension. The properties of the meshes and liquids are listed in Table 1.

Table 1 Mesh characteristics (a) and liquid properties (b).

a)

Sample number	Pore diameter (µm)	Wire diameter (µm)
1	25	25
2	50	36
3	80	50
4	100	65
5	150	100
6	200	125
7	250	100
8	400	220

b)

Liquid	Density (kg/m^3)	Viscosity (mPa s)	Surface tension (N/m)
Water	996	1	0.073
Acetone	793	0.30	0.023
20 %Water & 80% Glycerol	1119	10	0.067

Two different needle sizes, 21 gauge (0.82 mm OD, 0.51 mm ID) and 26s gauge (0.47 mm OD, 0.13 mm ID) were used to produce the drops and vary their diameter. Droplet impact velocity was varied from 2 m/s to 4 m/s by adjusting the height of release of the droplet above the mesh between 20 cm and 80 cm. The droplets fell under the influence of gravity. To confirm repeatability, droplet impacts were repeated at least 5 times for each set of impact conditions. Two different set-up configurations were used repeating the same group of experiments. In the first configuration, to focus exclusively on the porosity of the mesh and to avoid flexing during droplet impact, the meshes were stretched on a flat surface made of stainless steel, and clamped using a steel ring. In the second configuration, a portion of the mesh was suspended using a ring with a 20mm inner diameter. It was observed that in particular at higher impact velocity, a small vertical movement of the mesh occurred after the impact of the droplet. In order to verify if the amplitude of the oscillation can influence the final outcome, we repeated some of the experiments using 2 more rings with diameters of 15 mm and 25 mm, which offered smaller and larger unclamped area for the suspended mesh compared to the original case.

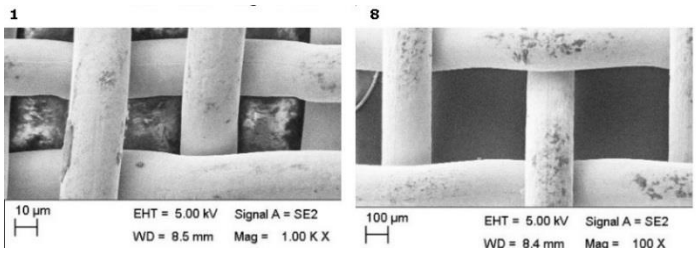

Fig. 1 SEM images of the stainless steel meshes sample number 1 and 8.

Droplet impacts were recorded using a Photron Fastcam SA4 high speed camera (with a resolution of 1024x800 pixels), angled at 60° to the horizontal plane in the case of the first configuration, and parallel to the plane in the case of the second configuration . The test area was illuminated using a custom-built high-speed LED light source synchronised to the high-speed camera. A purpose-built image processing algorithm was developed using MATLAB to measure the droplet initial diameter and the maximum spreading area of the impact. Impact velocity was also determined by measuring the rate of displacement of the droplet's centre of mass from the video images.

Results and Discussion

By observing the result of the experiments, it is finally possible to identify 6 different outcomes. For a lower impact velocity, these outcomes are: deposition, partial imbibition, and mesh penetration (Figure 2). While penetration occurs during impact and mainly as a result of the inertial force (higher impact velocity) and larger pore dimension, the partial imbibition occurs during the recoiling phase and is related to capillary force.

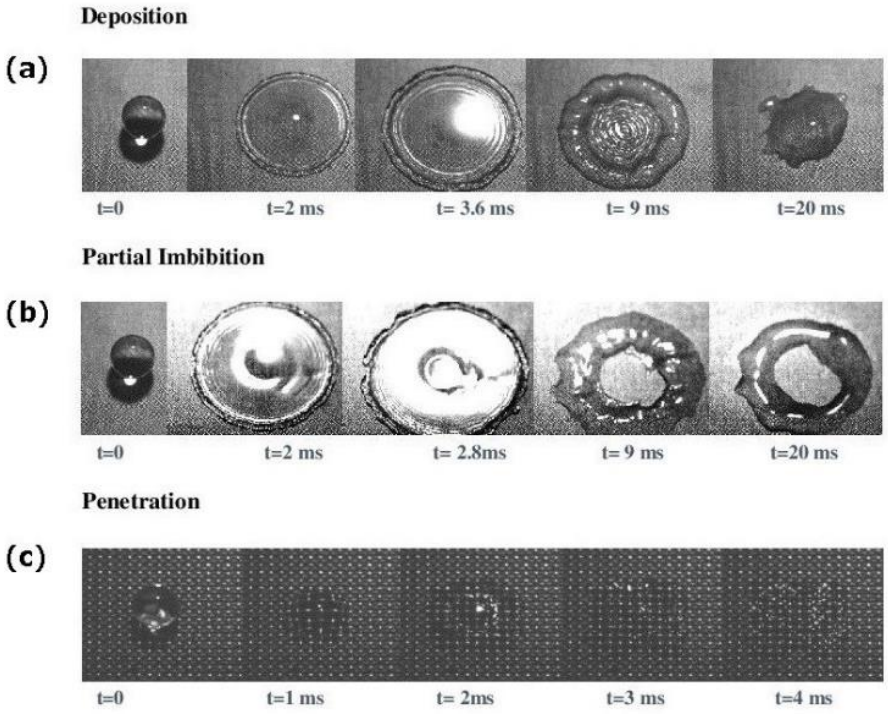

Figure 2 Impact outcomes for water droplets. **(a)** Deposition: $v_\mathrm{i} = 1.73$ m/s, $d = 3.06$ mm, $D_\mathrm{p} = 25$ µm, $D_\mathrm{w} = 25$ µm **(b)** Partial imbibition: $v_\mathrm{i} = 2.81$ m/s, $d = 1.96$ mm, $D_\mathrm{p} = 25$ µm, $D_\mathrm{w} = 25$ µm **(c)** Penetration: $v_\mathrm{i} = 1.96$ m/s, $d = 3.0$ mm, $D_\mathrm{p} = 400$ µm, $D_\mathrm{w} = 220$ µm

For a higher impact velocity, it is possible to observe a transition to a splash regime, which is still characterised by a final deposition, a partial imbibition and a penetration. In Figure 2, the time scale shows that the deposition and the partial imbibition are processes that take place in approximately 20 ms, whereas the penetration timescale is much shorter (~4 ms) as it is initiated during the impact itself. Liquid penetration can also affect droplet spreading on top of the mesh. Impact dynamics were observed for droplets landing on three meshes with different pore dimensions (25, 100 and 200 µm) at three different impact velocities (1.8 m/s, 2.9 m/s and 3.9 m/s). In order to describe the evolution of spreading with time, the standard dimensionless diameter and time were used, which are given by

$$D^* = \frac{d(t)}{d} \qquad t^* = t \cdot \frac{v_\mathrm{i}}{d}$$

Where d is the droplet initial diameter, $d(t)$ the evolution of the diameter in time after the impact and v_i the impact velocity [13].

Figure 3 (a) shows the spreading diameter for water droplets on a 25 µm mesh at three different velocities. The standard deviation on the maximum spreading diameter considering the three different velocities from the lowest to the highest is given respectively by 0.14, 0.17, 0.39. The spread factor increases with impact velocity, as is normally observed for droplet impact on a solid surface. Table 3 lists the values of *We* for each of these velocities. For a 25 µm mesh *We* is always less than the critical value of 8, implying that there is no penetration into the

mesh. Droplet impact dynamics are similar to those seen on an impermeable surface. The equation describing the spreading evolution on a smooth surface is given by

$$D_{max} = \frac{\sqrt{We + 12}}{3(1 - cos\theta_a) + 4(\frac{We}{\sqrt{Re}})}$$

Were θ_a is the dynamic contact angle after the spread and D_{max} the maximum spreading diameter. [14]. In the specific case, considering a water droplet of 3mm diameter and three velocity impact of 1.8; 2.9 and 3.9 m/s, the maximum spreading diameter on a smooth stainless steel surface, would be given respectively by 4, 4.6 and 5. The difference in maximum spreading diameter for a smooth surface and a porous surface will increase, increasing the size of the pores and the wire that consequently leads to a greater roughness.

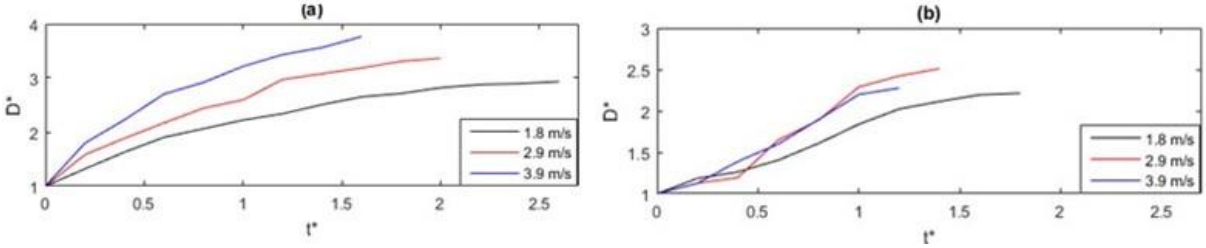

Figure 3 Evolution of dimensionless spreading diameter with time for water droplets with $d = 3$ mm. **(a)** $D_\mathrm{p} = 25$ µm, $D_\mathrm{w} = 25$ µm, **(b)** $D_\mathrm{p} = 200$ µm, $D_\mathrm{w} = 125$ µm.

Figure 3 (b) shows droplet impact on a mesh with 200 µm pores. The standard deviation on the maximum spreading diameter considering the three different velocities from the lowest to the highest is given respectively by 0.05, 0.01, 0.07. At the lowest velocity (1.8 m/s), the maximum spread factor is approximately 2.2, lower than it was on a the 25 µm mesh. The weaker spread can be explained by two different reasons: (i) for a larger pore size, a higher percentage of liquid will penetrate below the surface leading to a lower spreading diameter; (ii) at a larger pore size corresponds also a larger wire diameter, consequently during the spreading, the greater "roughness" will enhance the viscous dissipation leading to a smaller spreading diameter. In fact, the 200 µm pore size mesh, is characterised by a wire diameter of 125 µm whereas the 25 µm pore size mesh has a wire diameter of only 25 µm. For a mesh with 200 µm pores and *We* = 9.1 at the lowest impact velocity, this is barely above the limit for penetration. The reduced droplet spreading in this case is therefore most probably the result of surface roughness due to the larger wire diameter. When impact velocity is increased to 2.9 m/s the droplet spread increases, though it is less than it was on a 25 µm mesh (compare Figure 3
a and b). For this case, *We* = 22.5 (Table 2) which implies a significant penetration of liquid into pores. A calculation of the volume of the voids in the mesh under the droplet at its maximum spread shows that it was approximately 48% of the initial droplet volume (Table 2), so a significant amount of liquid can be trapped into the pores. At the highest impact velocity, $v_\mathrm{i} = 3.9$ m/s, the spreading of the droplet is slightly less than with an impact velocity of 2.9 m/s. For this case, *We* = 41.5, we have therefore a significant partial penetration into the pores. The loss of liquid, which could be as high as 38% of the initial droplet volume, would result in a smaller maximum spread diameter.

Table 2 Percentage of liquid penetration for water.

Experiment N	v_i (m/s)	We	D_{max} (mm)	D_w(mm)	D_p(mm)	Void volume %
1	1.8	1.1	8.6	0.025	0.025	12
2	2.9	2.8	9.8	0.025	0.025	16
3	3.9	5.2	10.8	0.025	0.025	20
4	1.8	4.6	6.4	0.065	0.1	20
5	2.9	11.2	7.7	0.065	0.1	29
6	3.9	20.8	7.0	0.065	0.1	24
7	1.8	9.1	6.2	0.125	0.2	36
8	2.9	22.5	7.2	0.125	0.2	48
9	3.9	41.5	6.4	0.125	0.2	38

In the case of a complete penetration, it is no possible to define a spreading of the droplet on the surface because the entire droplet penetrates inside the pore after the first millisecond. Considering the instant in which the droplet touches the surface, the time required for the first half of the spherical droplet to penetrate inside the surface will be given by

$$t_\mathrm{p} = \frac{d}{2v_\mathrm{i}}$$

Once the first half of the droplet penetrates inside the mesh, no spreading is detectable and penetration occurs. This leads to a dimensionless time equal to:

$$t_{\mathrm{p}}^{*} = \frac{t_{\mathrm{p}} v_{\mathrm{i}}}{d} = \frac{1}{2} = 0.5$$

If $t^{*} > 0.5 = t_{p}^{*}$: The spreading of the droplet will occur and, depending on the pore diameter there will be a partial imbibition of the liquid inside the surface,

If $t^{*} < 0.5 = t_{p}^{*}$: All the liquid will penetrate inside the surface without leading to any spreading.

Having a different time scale, it was chosen to define separately the transition between deposition and partial imbibition and the deposition and penetration in two regimes maps. In order to define the different regimes, a geometrical parameter was introduced, given by the ratio of the empty area over the full area of the mesh pore

$$\gamma = \frac{A_{full}}{A_{empty}} = \frac{(D_p + D_w)^2}{D_P^2} = D_p^2 \cdot \frac{\left(1+\frac{D_w}{D_p}\right)^2}{D_p^2} = \left(1 + \frac{D_w}{D_p}\right)^2$$

In fact, considering the spreading analysis it is clear that not only the pore diameter plays a role in the penetration of the liquid but also the wire diameter which will influence the percentage of liquid penetration and the void volume measure. In the case of partial imbibition, a larger dimension of the wire will lead to a higher liquid imbibition. In the case of penetration, a larger wire diameters and larger pore dimensions will lead to the complete penetration of the liquid below the surface.

Case $t^{*} < t_{p}^{*}$

For dimensionless times lower than t_{p}^{*}, drop penetration may occur. The regime map in Figure 4 shows the separation between deposition and penetration.

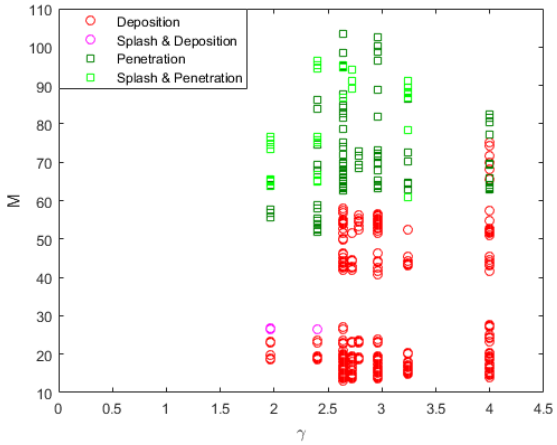

Figure 4 Regime distribution for all the liquids as a function of γ and M, transition between deposition and penetration.

The Weber number alone was not to sufficient to obtain a satisfactory description of outcome distribution. Therefore, the Weber was coupled with the Reynolds number, to capture the viscosity effects. The best choice of the parameter on y-axis was evaluated by:

$$M = \frac{Re^3}{\sqrt[2]{We}}$$

The transition with the penetration regime begins at M>50 until penetration becomes the only dominant outcome for M>80.

Case $t^{*} > t_{p}^{*}$

For $t^{*} > 0.5$, it is possible to observe the spreading of the droplet on the surface and consequently the complete penetration does not occur. Viscosity plays a major role to describe the deposition/partial-imbibition transition for which reason the parameter on the y axis is exclusively given by the Reynolds number in Figure 5. Increasing the viscosity and for lower Reynolds number, the dominant outcome is deposition. The transition between deposition and partial imbibition will be mainly influenced by a higher velocity or a lower viscosity. Higher values of Re (Re>10000) lead to a splash outcome.

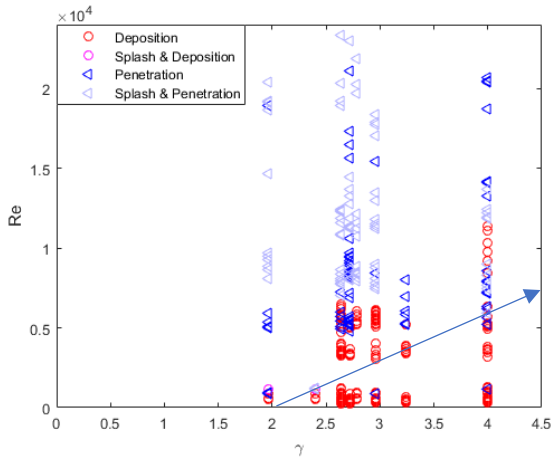

Figure 5 Regime distribution for all the liquids as a function of γ and Re with the transition between deposition and imbibition

Our result show that, in contradiction to the findings of Roisman et al. [7], the two most important parameters to describe the impact of droplets on a porous material may not be the Weber number and a ratio given by considering the geometrical roughness. The present results show a good agreement with those of Neyval et al. [9] and Sahu et al. [10], considering respectively the major role given to the surface tension, and the fact that an imbibition outcome is mainly observable for droplets with a larger diameter.
The second configuration of the suspended meshes leads to similar outcomes which are shown in Figure 6.

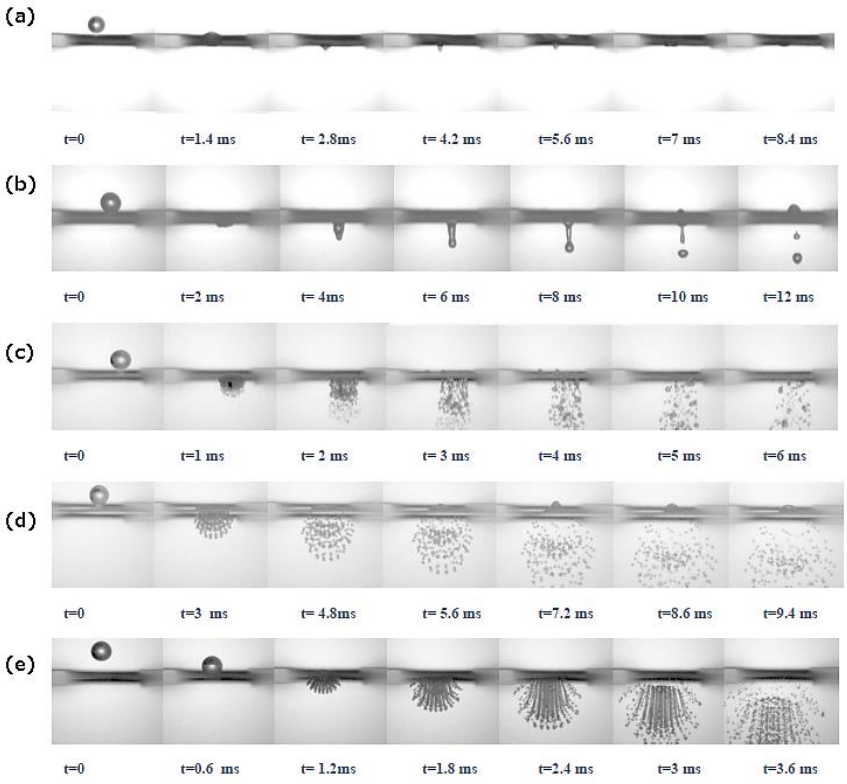

Figure 6 (a) Deposition Outcome; Water & Glycerol, v_i= 1.8 m/s, d= 2.8 mm, D_p= 25µm, D_w= 25µm **(b)** Partial Imbibition Outcome. Water, v_i= 1.8 m/s, , d= 2.8 mm, D_p= 50µm, D_w= 60µm **(c)** Partial Imbibition Outcome; Water, v_i= 3.6 m/s, d= 3.0 mm, D_p= 50µm, D_w= 60µm **(d)** Partial Imbibition Outcome; Water, v_i= 1.8 m/s , d= 2.9 mm, D_p= 400µm, D_w= 220 µm **(e)** Penetration Outcome; Water, v_i=3.6 m/s, , d= 2.9 mm, D_p= 400µm, D_w= 220 µm

In the sequence in Figure 6. (a) it is possible to observe the impact of a droplet of glycerol/water mixture on a surface with pore size of 25 µm at a velocity of 1.8 m/s. Due to the high viscosity of the liquid, the small dimension of the pore and the low velocity, no penetration of the liquid occurs and the outcome is defined as deposition.

However, in Figure 8 (b-c) the sequences show a partial imbibition outcome. In both cases the impact is given by a droplet of water on a surface with porosity of 50 µm. Whereas in Figure 6.b, due to the lower velocity of 1.8 m/s, the liquid which penetrates below the surface separates from an initial liquid jet leading to the formation of 2 droplets. In Figure 6.c, due to the higher velocity of 3.6 m/s, no liquid jet is observed and the liquid which penetrates below the surface forms a spray-cone composed by a high number of very small size droplets. A similar situation is observable in Figure 6.d-e. The sequences show the impact of a droplet of water on a surface of 400 µm porosity. In Figure 6.d due to the lower velocity of 1.8 m/s, the outcome is a partial imbibition, in fact part of the liquid remains above the surface after the impact whereas in Figure 6.e the outcome is penetration due to the higher velocity of 3.6 m/s. The penetration of the liquid after the impact is influenced by the impact velocity, as it is shown in Figure 6.b-c or Figure 6.d-e, in which, for the same pore size, a higher velocity leads to a different effect in terms of liquid penetration. Pore size plays an important role as well, in fact comparing Figure 6. (b) with Figure 6. (d), it is possible to observe that, given the same impact velocity but increasing the pore size, a different effect is achieved and the percentage of liquid penetration will increase with pore diameter.
An estimation of the liquid penetration is given, computing the volume of the single droplets ejected from the surface after the impact (case of Figure 6 b) or subtracting the volume of the remaining cap above the mesh from the initial volume (case of Figure 6 a-c-d). The initial volume of the droplet is calculated from the droplet radius, assuming that the droplet has a perfectly spherical shape. The general trend of liquid penetration, in function of pore size, liquid properties and impact velocity is shown in Figure 7. In Figure 7 (a), it is shown that increasing the pore size the percentage of liquid penetration will increase. At the same time, given the same pore size but increasing the impact velocity, the percentage of liquid penetration will be higher. Figure 7 (b), shows the trend of liquid penetration for the three liquids at the same impact velocity. It is shown that given the same pore size and velocity, increasing the viscosity, the liquid penetration will be smaller. At the same time, for a smaller surface tension, as for the case of acetone, given the same pore size and velocity, the percentage of penetration will be higher. In order to verify if the vertical movement of the mesh due to the impact may influence the percentage of penetration or the outcome, some of the experiments were repeated with water on surfaces with pore sizes of 25, 200 and 400 µm. No significant difference was observed in terms of outcome and percentage penetration of the liquid (Table 3). It is possible to conclude that the movement of the mesh has no relevant effect on the nature of the outcome.

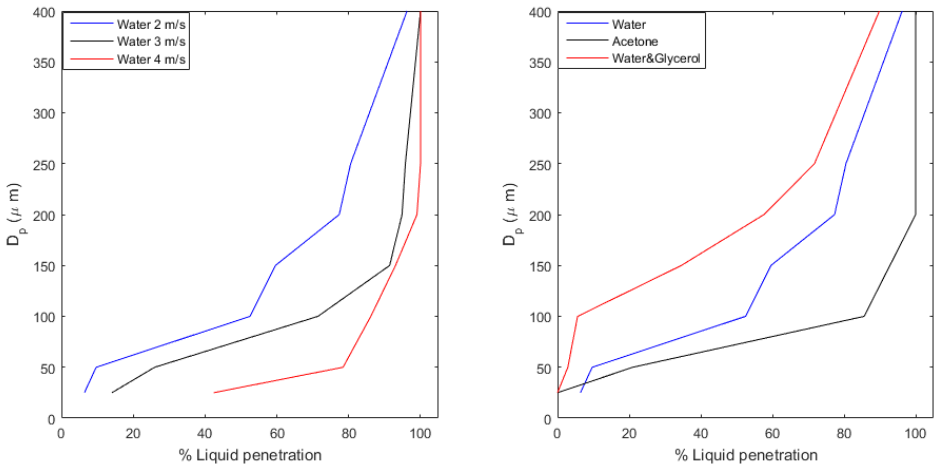

Figure 7 (a) Percentage of liquid penetration of water in function of pore size given different range of impact velocity (b) Percentage of liquid penetration of water, acetone, water & glycerol at 2 m/s impact velocity in function of pore size.

Table 3 Percentage of liquid penetration for different ring size

Pore size (μm)	Impact velocity (m/s)	% Liquid penetration ring size (1.5cm)	% Liquid penetration ring size (2 cm)	% Liquid penetration ring size (2.5cm)
25	2	7	10	7
25	3	13	11	14
25	4	46	42	43
200	2	79	76	77
200	3	90	88	95
200	4	100	98	99
400	2	96	94	96

The result presents a good agreement with Lorenceau et al. [11], in fact, given the same pore dimension but increasing the velocity a transition occurs between an outcome for which the liquid is captured by the surface or partially penetrate inside the pore.

Conclusions

This study is focused on the investigation of droplet impact on metallic meshes with a wide range of pore sizes. It was found that the attempt to represent the different outcome regimes excluding a geometrical parameter referred to mesh wire diameter was not satisfactory to obtain a proper identification of the impact regimes. In addition, to achieve a clear distinction of the impact regimes between deposition and penetration, it is fundamental to consider a dimensionless number which takes account the liquid properties, specifically, the viscosity and the surface tension. To reflect the above points, new dimensionless parameters, $\boldsymbol{M}$ and γ, were introduced, and the outcomes of the impact are predicted for the present range of experimental parameters. No splash outcome was observed in the case of the suspended meshes. It was confirmed that the liquid properties and the geometry of the meshes play a role in the definition of the outcome and influence the impregnation properties of the mesh.

Acknowledgements

The authors would like to thank Prof. Morgan Heikal, Chair of the Advanced Engineering Centre in Brighton, to agree the fund for Chandra's Visiting Professorship.

References

[1] Yarin A L, "Drop impact dynamics: Splashing, spreading, receding, bouncing," *Annual Review of Fluid Mechanics,* vol. 38, pp. 159-192, 2006.

[2] Bertola V, "Some applications of controlled drop deposition on solid surfaces," *Recent Patents on Mechanical Engineering,* vol. 1, pp. 167-174, 2008.

[3] Weclas M, "Potential of porous media combustion techonology as applied to internal combustion engines," *Journal of Thermodynamics,* vol. 2010, p. 39 pages, 2010.

[4] Ping H, Ying L, Rui Q., "Fluid dynamics of the droplet impact processes in cell printing," *Microfluid Nanofluid,* vol. 18, pp. 569-585, 2015.

[5] Woo Shik Kim, Sang Yong Lee., "Behaviour of drop impinging on heted porous surfaces," *Experimental Thermal and Fluid Science,* vol. 55, pp. 62-70, 2014.

[6] Chandra S, Avedisian C T., "Observation of droplet impingement on a cermaic porous surface," *Int. J. Heat Mass Transfer,* vol. 10, pp. 2377-2388, 1992.

[7] Roisman I V, Lembach A, Tropea C, "Drop splashing induced by target roughness and porosity: the size plays no role," *Advanced in Colloid and Interface Science,* vol. 222, pp. 615-621, 2015.

[8] Yamamoto K, Takezawa H, Ogata S., "Droplet impact on textured surfaces composed of commercial stianless razor baldes," *Colloids and Surfaces ": Physicochemical and Engineering Aspcects,* vol. 506, pp. 363-370, 2016.

[9] Neyval C R JR, Griffiths R F, Santos J M., "Numerical simulation of the impact of liquid droplets on porous surfaces," *Jorunal of computationl Physics,* vol. 198, pp. 747-770, 2004.

[10] Sahu R P, Sett S, Yarin A L, Pourdeyhimi B, "Impact of aqueus suspension drops onto non-wettable porous membranes: Hydrodynamics focusing and penetration of nanoparticles," *Colloids and Surfaces A: Physicochem, Eng, Aspects,* vol. 467, pp. 31-45, 2015.

[11] Lorencueau E, Quéré D., "Drops impacting a sieve," *Journal of Colloid and Interface Science,* pp. 244-249, 2003.

[12] Delpos A, Lorenceau E, Pitois O., "Forced Impregation of a capillary tube with drop impact," *Journal of Colloid and Interface Science,* pp. 171-177, 2009.

[13] R Rioboo., M. Marengo, C Tropea., "Time evolution of liquid drop impact onto solid, dry surfaces," *Exp. Fluids,* vol. 33, pp. 112-124, 2002.

[14] Pasandideh-Fard M, Qiao Y. M., Chandra , Mostaghimi J., "Capillary effects during droplet impact on a solid surface," *Physic of Fluids,* vol. 8, 1996.